

## LAMINATE CHARACTERIZATION OF FIBER-REINFORCED POLYMER COMPOSITES BY MICRO-COMPUTED TOMOGRAPHY

M. Mühlstädt<sup>1\*</sup>, S. Maenz<sup>1</sup>, R. Ramm<sup>2</sup>, P. Kühmstedt<sup>2</sup>, K. D. Jandt<sup>1</sup>, J. Bossert<sup>1</sup>

<sup>1</sup>*Institute of Materials Science and Technology, Department of Physics and Astronomy, Friedrich Schiller University Jena, Löbdergraben 32 in 07743 Jena (Germany)*

<sup>2</sup>*Fraunhofer Institute for Applied Optics and Precision Engineering IOF, Albert-Einstein-Str. 7 in 07745 Jena (Germany)*

\* e-mail address of the corresponding author: [mike.muehlstaedt@uni-jena.de](mailto:mike.muehlstaedt@uni-jena.de)

**Keywords:** Micro-Computed Tomography; Polymer Matrix Composites (PMC); Mechanical testing; Resin Transfer Molding (RTM).

### Abstract

*The aim of this study was the determination of the geometric structural parameters of a glass textile reinforcement, which is embedded into an epoxy polymer matrix, by micro-computed tomography ( $\mu$ CT). Therefore, four different glass fabrics were investigated. The  $\mu$ CT images of the composites feature a good contrast between glass reinforcement and polymer matrix. The resolution is high enough for the determination of the geometric structural parameters: wavelength of warp and fill yarn, amplitude of warp and fill yarn, width of warp and fill yarn, height of warp and fill yarn and the gap between two adjacent warp and fill yarns. The micro-computed tomography shows a high potential for an efficient measurement of the three dimensional geometric structural properties of laminated woven textile fabrics.*

### 1 Introduction

Fiber-reinforced polymer composites (FRPC) feature outstanding material properties, like high specific strength and specific modulus of elasticity as well as a high anisotropy. Mechanical and physical properties can be adjusted to technical requirements by an individual composite design, i.e. a variation of the fiber's or the fabric's orientation. Of particular interest are fabrics with a definite structure property relationship, as it can be found for nonwoven and woven fabrics. Nonwoven fabrics like unidirectional or bidirectional fabrics have a quite simple structure property relationship: The filaments within the rovings are straight aligned in one or respectively two directions. The structure relationship of woven fabrics is more complex because of an additional undulation of the rovings perpendicular to the fabric layer. In order to optimize load-bearing components to specific applications simulation techniques have to be applied, e.g. micromechanics and finite element simulation (FES). Commercially available software solutions for the simulation of construction parts made of textile fabrics require the material properties of the laminated fabric, i.e. ANSYS Composite PrepPost. Other software solutions, for example ESAComp, can partially calculate these properties by using different micromechanical models.

The properties, arising for a laminated unidirectional nonwoven fabric can be calculated by the use of simple micromechanical models, i.e. Voigt bounds[1] and Reuss bounds[2], Chamis[3], Hashin[4,5] and Halpin-Tsai[6]. Laminated woven fabrics are more sophisticated.

This concerns the model as well as the modeling of the fabric. First models were developed by Ishikawa and Chou [7,8]. They proposed a one dimensional mosaic model by modeling the warp and fill yarn as unidirectional [7]. Later models of Ishikawa and Chou also include a more accurate modeling of the warp yarn, the so-called undulation model. However, the fill yarn was not modeled [8]. Naik and Shembekar [9] developed a two dimensional woven fabric model, which models fill and warp yarn using a sinusoidal shape function. In the recent years different improvements concerning these models and other models were developed [10-13]. Indeed, all these models are based on a modeling of the yarn geometry and assume a unidirectional fiber orientation within infinitesimal yarn volume elements. Thus, it is necessary to get information about the three dimensional geometrical structure of the fill and warp yarns within the laminated fabrics of such a composite construction part. Figure 1 illustrates, which geometric structural parameters are required for the model presented by Naik and Shembekar.

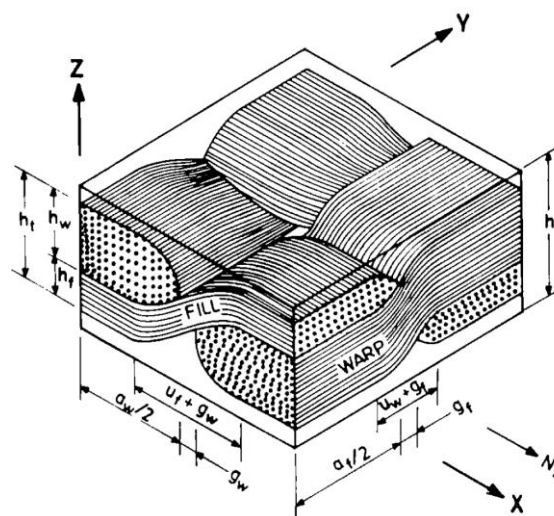


**Figure 1.** Schematic illustration of the geometric structural parameters.  $h$  is the height of a representative unit cell of a woven fabric,  $h_w$  is the height of the warp yarn,  $h_f$  is the height of the fill yarn,  $g_w$  and  $g_f$  are the gaps between two adjacent warp yarns respectively fill yarns,  $a_w$  and  $a_f$  denote the width of the warp respectively the fill yarn and  $u_w$  and  $u_f$  are assigned with the undulation of the warp yarn respectively the fill yarn [9].

It is of importance to determine these geometric structural parameters of the laminated woven fabric, due to occurring changes of the fabric during draping and infiltration. These geometric structural parameters can be obtained by the analysis of microsections of the composite and an imaging by light microscopy or scanning electron microscopy. However, both methods have the disadvantage that only a small two dimensional segment of the whole composite is present. One single two dimensional image cannot reveal all required geometric structural parameters. Moreover, the sample preparation is time consuming and expensive, due to the required sandpaper and polishing agent. The micro-computed tomography ( $\mu$ -CT) offers a non-destructive method for the examination of FRPCs. Due to the difference in the X-ray absorption coefficients of the glass reinforcement and the polymer matrix it is possible to get a three-dimensional mapping of the yarns' on the micro-scale. Moreover, the process directly yields a three-dimensional computer-aided design (CAD) model for further analysis, i.e. FES.

## 2 Materials and Testing Methods

### Materials

In this study, CR81/CH81-6 (Sika Deutschland GmbH, Stuttgart, Germany) was used as the resin system. The resin and the hardener were mixed in the preset relation of 100 to 30 wt%. As reinforcement four different woven glass textiles were used, obtained from TISSA (TISSA, Glasweberei AG, Oberkulm, Switzerland). These four glass textiles are listed in Table 1.

	material A	material B	material C	material D
TISSA article number	11896	13236	15136	13458
weaving	plain	plain	plain	twill 1/3
thickness [mm]	0.30	0.30	0.30	0.29
weight [g/m <sup>2</sup> ]	285-315	237-263	323-357	293-323
number of warp yarns [yarns/cm]	12.00	6.00	5.80	12.00
number of fill yarns [yarns/cm]	12.00	6.00	5.80	10.00

**Table 1.** Properties of the glass textile fabrics according to manufacturer's data.

Priming wax (R&G GmbH, Waldenbuch, Germany) was used as the release agent for the silicone mold.

### Sample Preparation

All laminates were prepared as follows. One layer of each glass textile was draped into a rectangular silicone mold and infiltrated by the epoxy resin system. After the infiltration the samples were cured for 12 h at 80°C.

### Micro-Computed Tomography

The cured FRPC samples were investigated by a v|tome|x  $\mu$ -CT system, equipped with a 180 kV nanofocus and a 240 kV microfocus tube (GE Sensing and Inspection Technologies GmbH, Wunstorf, Germany). The smallest attainable voxel size is about 3  $\mu\text{m} \times 3 \mu\text{m} \times 3 \mu\text{m}$ . For this study the 240 kV microfocus tube was used at 50 kV and 340  $\mu\text{A}$ . The applied integration time was 1000 ms. The resulting voxel size was 17.5  $\mu\text{m} \times 17.5 \mu\text{m} \times 17.5 \mu\text{m}$ . The analysis of the  $\mu$ -CT data was performed by using 3D analyzing Software VG STUDIO MAX 2.1 (Volume Graphics GmbH, Heidelberg, Germany) and MAVI 1.4 (Fraunhofer ITWM, Kaiserslautern, Germany).

### Determination of the Fabric Geometric Structural Parameters

In the following it will be illustrated how the geometric parameters of the laminated woven fabric were determined from the  $\mu$ -CT images. The following parameters need to be known for the micromechanical model presented by Naik and Shembekar [9]: the amplitude of the warp and fill yarn, the wavelength of the warp and fill yarn, the height of the warp and fill yarn, the width of the warp and fill yarn, as well as the gap between two adjacent warp and fill yarns. In the first step, the coordinate system was defined. The plain, defined by the woven fabric was declared as the xy-plain. The direction of the x-axis was defined by the fill yarn. The height of the yarns was determined by selecting an area, where only the fill or the warp yarn is present, see Figure 1. Afterwards, two parallel lines were fitted to the widest part of the yarn section. The resulting distance between these lines is assigned with the height of the yarn.

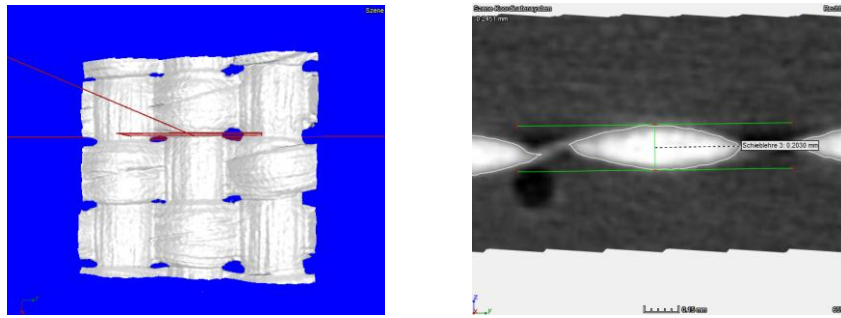


**Figure 1.** Determination of the fill yarn height from a  $\mu$ -CT image. The left figure illustrates the xy-plane and the position of the yz-plane, which is illustrated on the right side.

The amplitude of the yarns was determined by measuring the distance between the top and the bottom of a yarn, see Figure 2. From this distance the height of the yarn was subtracted. The amplitude of the yarn was gained by dividing this result by two. The wavelength of the fill yarn can be determined by measuring the distance between the middle of a warp yarn and the middle of the adjacent warp yarn, see Figure 2.

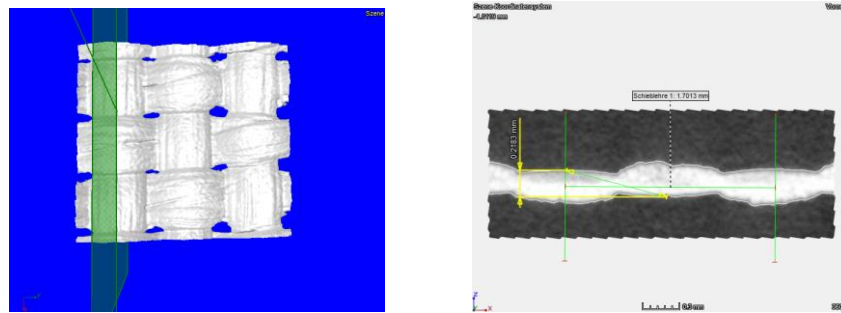


**Figure 2.** Determination of the fill yarns amplitude and wavelength from a  $\mu$ -CT image. The left figure shows the xy-plane and the position of the xz-plane, which is illustrated on the right side.

For the determination of the yarn width two lines describing the extension of the yarn in the width were fitted to the yarn. The distance, perpendicular to the yarn direction, between these parallel lines is the yarn width, illustrated in Figure 3.

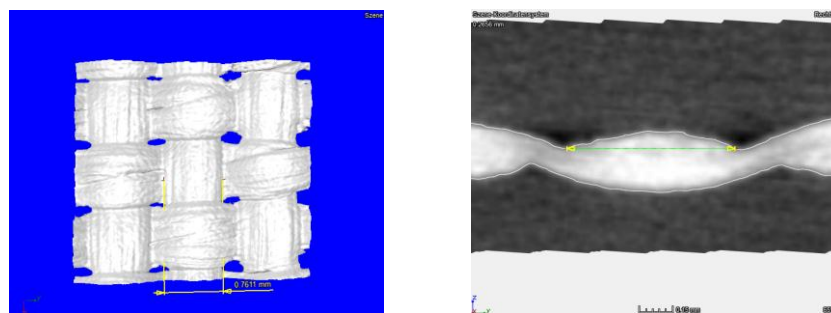


**Figure 3.** Determination of the fill yarn width from a  $\mu$ -CT image. The left figure shows the xy-plane and the right figure the yz-plane.

Figure 4 illustrates the determination of the gap between two adjacent fill yarns. One set of two parallel lines, limiting the gap at its widest extension, were fitted to two adjacent yarns. The distance between both lines, perpendicular to the yarn direction, is assigned with the so-called yarn gap.

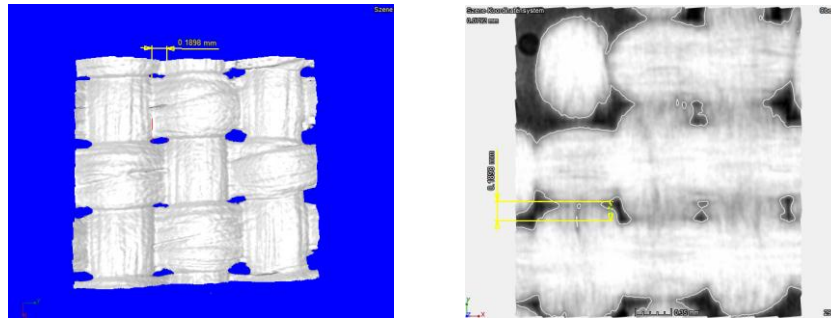


**Figure 4.** Determination of the fill yarn gap of two adjacent fill yarns from a  $\mu$ -CT image. The left and the right figure show the xy-plane.

### 3 Results

For the determination of the geometric structural parameters the prepared laminates were investigated using the  $\mu$ -CT. Figure 5 shows the xy-plane of a preselected area of each sample studied by  $\mu$ -CT. The gray values have been fixed at a level so that only the glass textile fabric stays present. The attained resolution of the  $\mu$ -CT images allows to partially observing single glass filaments on the surface of the yarns. However, the right image on Figure 2 and the right image on Figure 3 show that it is not possible to clearly separate the fill yarn and the warp yarn from each other.

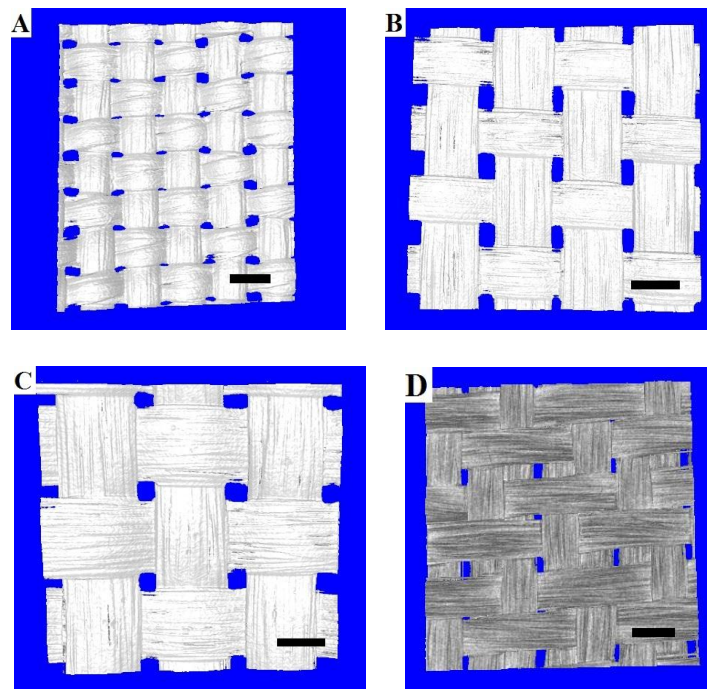


**Figure 5.** Illustration of the xy-plane of the  $\mu$ -CT images of the four different fabrics used in this study. Image A belongs to material A, image B to material B, image C to material C and image D to material D (see table 1). The grayscale indicates the glass textile fabric and the blue color the auto background color of the software. Scale 1mm.

The measured geometrical structural parameters: wavelength of warp and fill yarn, amplitude of warp and fill yarn, width of warp and fill yarn, height of warp and fill yarn and the gap between two adjacent warp and fill yarns are listed in Table 2. Furthermore, the standard deviation is given for each value.

	material A	material B	material C	material D
wavelength warp yarn [mm]	$2.02 \pm 0.08$	$3.39 \pm 0.11$	$3.50 \pm 0.10$	$3.25 \pm 0.05$
wavelength fill yarn [mm]	$1.70 \pm 0.05$	$3.36 \pm 0.07$	$3.46 \pm 0.07$	$4.07 \pm 0.06$
amplitude warp yarn [mm]	$0.10 \pm 0.02$	$0.07 \pm 0.02$	$0.09 \pm 0.02$	$0.06 \pm 0.01$
amplitude fill yarn [mm]	$0.03 \pm 0.02$	$0.03 \pm 0.02$	$0.04 \pm 0.03$	$0.08 \pm 0.02$
width warp yarn [mm]	$0.89 \pm 0.06$	$1.19 \pm 0.06$	$1.46 \pm 0.07$	$0.80 \pm 0.05$
width fill yarn [mm]	$0.79 \pm 0.03$	$1.41 \pm 0.11$	$1.40 \pm 0.06$	$0.81 \pm 0.05$
height warp yarn [mm]	$0.14 \pm 0.02$	$0.14 \pm 0.01$	$0.18 \pm 0.01$	$0.16 \pm 0.02$
height fill yarn [mm]	$0.18 \pm 0.02$	$0.14 \pm 0.02$	$0.22 \pm 0.01$	$0.16 \pm 0.02$
gap between warp yarns [mm]	$0.16 \pm 0.05$	$0.59 \pm 0.03$	$0.35 \pm 0.03$	$0.44 \pm 0.07$
gap between fill yarns [mm]	$0.26 \pm 0.04$	$0.35 \pm 0.09$	$0.39 \pm 0.05$	$0.23 \pm 0.03$

**Table 2.** Geometric structural parameters and the corresponding standard deviations of the four different woven textile glass reinforcements.

In order to get some comparable values the wavelengths of the warp and the fill yarns of the four different materials were converted into the yarns per unit length. Based on the measured wavelength the yarns per unit length of the warp and the fill yarn were calculated. The calculation of the yarns per unit length considers that for a plain weave fabric one single wavelength comprises two yarns and for the twill 1/3 weave fabric four yarns. The results are listed in Table 3.

	material A	material B	material C	material D
warp yarn [yarns/cm]	$9.90 \pm 0.39$	$5.89 \pm 0.19$	$5.71 \pm 0.17$	$12.32 \pm 0.21$
fill yarn [yarns/cm]	$11.73 \pm 0.33$	$5.96 \pm 0.12$	$5.78 \pm 0.11$	$9.83 \pm 0.14$

**Table 3.** Yarns per unit length of the warp and the fill yarn for the four fabrics.

#### 4 Discussion

The difference between the absorption coefficients of the glass of the reinforcing textiles and that of the polymer matrix result in a good visibility of the embedded glass fabric. However, there is no contrast between two intersecting warp and fill yarns. This is due to the resolution limit of the  $\mu$ -CT technology of approximately  $1 \mu\text{m} \times 1 \mu\text{m} \times 1 \mu\text{m}$  [14]. So that it is not possible to separate two closely together lying yarns, i.e. at the intersection points of the weaving. The same problem will be expected for composites with a multi-layered fabric stack-up. For this reason we prepared samples with a single fabric layer at first.

The measurement of the wavelength of the warp and the fill yarn of material A were found to be  $(2.02 \pm 0.08)$  mm and  $(1.70 \pm 0.05)$  mm, respectively. These wavelengths result in  $(9.90 \pm 0.39)$  yarns/cm for the warp yarn and  $(11.73 \pm 0.33)$  yarns/cm for the fill yarn. Material B has a warp yarn wavelength of  $(3.39 \pm 0.11)$  mm and a fill yarn wavelength of  $(3.36 \pm 0.07)$  mm. These wavelengths result in  $(5.89 \pm 0.19)$  yarns/cm for the warp yarn and  $(5.96 \pm 0.12)$  yarns/cm for the fill yarn. For material C the wavelength of the warp yarn is  $(3.50 \pm 0.10)$  mm and for the fill yarn it is  $(3.46 \pm 0.07)$  mm. Thus, there are  $(5.71 \pm 0.17)$  warp yarns per cm and  $(5.78 \pm 0.11)$  fill yarns per cm. The twill 1/3 weave fabric showed a warp yarn wavelength of  $(3.25 \pm 0.05)$  mm and a fill yarn wavelength of  $(4.07 \pm 0.06)$  mm. Thus, the calculated values of material B, material C and material D fit very well with the manufacture's data. Only, for the warp yarn of material A larger deviations from the manufacture's data are present. A reason for this could be a shift of the yarns during the draping of the fabric and the subsequent infiltration process.

Moreover, the analysis of the  $\mu$ -CT measurements results in small standard deviations of the analyzed geometric structural parameters of the fabrics. This means, on the one hand, that the  $\mu$ -CT method has enough precision for the present study. On the other hand it indicates that the structure of the fabric is homogeneously distributed across the layer.

## 5 Conclusion

In the present study four different woven glass fabrics were embedded into an epoxy polymer matrix and investigated concerning the geometrical structure of the yarns by  $\mu$ -CT. The  $\mu$ -CT could well reveal the geometrical structure of the yarns within the laminated glass textile reinforcements. Thus, the  $\mu$ -CT emerges as a promising technology for the analysis of composites. The determination of the geometric structural parameters, which are necessary for a modeling of the fabric's geometric structure, was done. The standard deviations are small, so that a simulation based on this data can give a trustable result. The next step need to be done is a simulation based on the outlined geometric structural parameters. A comparison of the simulation results and the mechanical properties measured by experiment is also planned. Furthermore, the determination of the geometric structural parameters of FRPCs will be enlarged to more complex fabric structures, i.e. more than one fabric layer.

## Acknowledgement

The study was financially supported by the Thüringer Aufbaubank (TAB) with the project FiLiMA (grant ID 2010 FE 9044) and the project mCT (grant ID 2009 FE 9111). All woven glass textile fabrics used in the present study were provided by the TISSA Glasweberei AG.

## References

- [1] Voigt W. Ueber die Beziehung zwischen den beiden Elastizitätsconstanten isotroper Körper. *Annalen der Physik*, **38**, pp. 573-587 (1889).
- [2] Reuss A. Berechnung der Fließgrenze von Mischkristallen auf Grund der Plastizitätsbedingung für Einkristalle. *ZAMM*, **9**, pp. 49-58 (1929).
- [3] Chamis C.C. Simplified Composite Micromechanics Equations for Hygral, Thermal and Mechanical Properties. *SAMPE Q*, **15(3)**, pp. 14-23 (1984).
- [4] Hashin Z., Rosen B.W. The Elastic Moduli of Fiber-Reinforced Materials. *ASME Journal of Applied Mechanics*, **31**, pp. 223-232 (1964).
- [5] Hashin Z. Analysis of Composite Materials – A Survey. *Journal of Applied Mechanics*, **50**, pp. 481-505 (1983).
- [6] Halpin J.C., Kardos J.L. The Halpin-Tsai Equations: A Review. *Polymer Engineering and Science*, **16(5)**, pp. 344-352 (1976).
- [7] Ishikawa Z., Chou T.-W. Elastic Behavior of Woven Hybrid Composites. *Journal of Composite Materials*, **16**, pp. 2-19 (1982).
- [8] Ishikawa Z., Chou T.-W. Stiffness and Strength Behaviour of Woven Fabric Composites. *Journal of Materials Science*, **17**, pp. 3211-3220 (1982).
- [9] Naik N.K., Shembekar P.S. Elastic Behavior of Woven Fabric Composites: I – Lamina Analysis. *Journal of Composite Materials*, **26**, pp. 2196-2225 (1992).
- [10] Vandeurzen Ph., Ivens J., Verpoest I. A Three-Dimensional Micromechanical Analysis of Woven-Fabric Composites: II. Elastic Analysis. *Composites Science and Technology*, **56**, pp. 1317-1327 (1996).
- [11] Ito M., Chou T.-W. An Analytical and Experimental Study of Strength and Failure Behavior of Plain Weave Composites. *Journal of Composite Materials*, **32**, pp. 2-30 (1998).

- [12] Scida D., Aboura Z., Benzeggagh M.L., Bocherens E. A Micromechanics model for 3D elasticity and failure of woven-fibre composite materials. *Composites Science and Technology*, **59**, pp. 505-517 (1999).
- [13] Donadon M.V., Falzon B.G., Iannucci L., Hodgkinson J.M. A 3-D micromechanical model for predicting the elastic behaviour of woven laminates. *Composites Science and Technology*, **67**, pp. 2467-2477 (2007).
- [14] Mizutani R., Takeuchi A., Osamura R.Y., Takekoshi S., Uesugi K., Suzuki Y. Submicrometer tomographic resolution examined using a micro-fabricated test object. *Micron*, **41**, pp. 90-95 (2010).